Springer

KSME

Journal of Mechanical Science and Technology 29 (5) (2015) 1913~1919
www.springerlink.com/content/1738-494x
DOI 10.1007/s12206-015-0413-6

Dynamic analysis of a megawatt wind turbine drive train †

Caichao Zhu[1,*], Shuang Chen[1], Chaosheng Song[1], Huaiju Liu[1], Houyi Bai[2] and Fei Ma[2]

[1] *The State Key Laboratory of Mechanical Transmission, Chongqing University, Chongqing, 400030, China*
[2] *Chongqing Wangjiang Industry Co., LTD, Chongqing, 400071, China*

(Manuscript Received July 21, 2014; Revised December 24, 2014; Accepted January 10, 2015)

Abstract

The dynamic performance of a wind turbine drive train significantly influences the operation of an entire machine. In this work, a megawatt wind turbine drive train is subject to theoretical and experimental dynamic analysis. The method of rigid-flexible coupling multibody dynamics was applied to develop a dynamic model of the entire drive train. This model was then used to study the natural characteristics of the system. The blades, hub, main shaft, and speed-up gearbox in the dynamic model were modeled as flexible bodies. The potential resonances of the system were detected through Campbell and modal energy distribution analyses. Theoretical results show that the first-order natural frequency of the system is approximately 1.72 Hz. This frequency represents a torsional vibration mode, Moreover, resonances are not observed within the normal operating speed range of the drive train. An experimental remote real-time system was developed to monitor the torsional vibration of the drive train. This vibration was used to measure the torsional vibration of the system overall. The experimental results are consistent with the theoretical results.

Keywords: Drive train; Dynamic behavior; Potential resonance; Torsional vibration test; Wind turbine

1. Introduction

Wind turbines mainly consist of an air-operated system, a drive train, an electrical set, and a control set. Given the time-varying wind load, faults in the drive train are observed more often than those in the other components of the machine [1, 2]. The typical drive train of a wind turbine is composed of a wind rotor, a main shaft, a speed-up gearbox, flexible couplings, and a generator [3, 4]. The drive train reflects nonlinear behavior and coupling effects because of its complicated structure [5-7]. The ranges of the operating speed and of the excitation frequency of the system are wide. The system may encounter resonances that cause significant vibration and affect the normal operation of the machine. Thus, the dynamic behavior of the drive train in the wind turbine must be clarified.

A number of studies have been conducted on the dynamic behavior of wind turbine drive trains. Stol presented the linear state-space representation of a wind turbine with generic, multiple degrees of freedom (MDOF) to test various control methods and paradigms. Moreover, this researcher extracted the necessary modal properties according to Floquet theory [8]. Nam et al. developed a drive train model for a multi-megawatt (MW) wind turbine and analyzed closed-loop dynamic characteristics for different torque schedules. Their results show that the slope of the torque for the rotor speed in the transient region is the major factor dictating the performance and mechanical loading of the wind turbine [9]. Helsen et al. investigated the effectiveness of three configurations on the dynamic behavior of a wind turbine gearbox using the flexible multibody technique. These configurations are the three-point mounting, double bearing configuration, and hydraulic damper system [10]. Burlibasa investigated in detail the dynamic properties in the frequency domain of a large wind system that operates under a full-load regime [11]. Song dynamically modeled a wind turbine drive train using flexible multi-body method. Specifically, the natural characteristics and vibration response were analyzed [12]. Peeters et al. applied the flexible multibody simulation technique to identify the internal dynamic behavior of a wind turbine and its drive train [13, 14]. Zhu et al. presented a dynamic model of a wind turbine gearbox with flexible pins to determine the influence of such pins on the dynamic characteristics of a wind turbine gearbox [15-17]. They also investigated the external excitations, internal excitations, and dynamic response of a MW wind turbine drive train [18]. ZF designed a test rig for a 13.2 MW wind turbine gearbox and developed a dynamic model for it using Simpack [19]. However, little research has been conducted on drive train dynamics to prevent resonance in wind turbines according to rigid-flexible coupling dynamic theory and with experimental verification.

*Corresponding author. Tel.: +86 23 65111192, Fax.: +86 23 65111192
E-mail address: cczhu@cqu.edu.cn
† Recommended by Associate Editor Cheolung Cheong

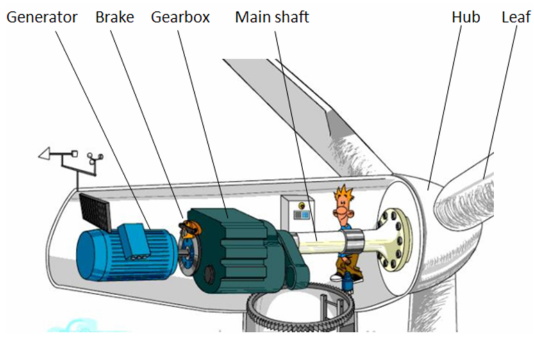

Fig. 1. Typical indirect driving wind turbine in a drive train.

In the current work, the theory of rigid-flexible coupling dynamics is applied to develop a MDOF dynamic model for a MW wind turbine drive train. The dynamic behavior of the system is studied theoretically and experimentally to guide the design optimization of the drive train of a wind turbine.

2. Basic structure and transmission principles of the drive train

Given different types of drive train, wind turbines can be classified into three types as well: the direct, indirect, and hybrid driving types [20, 21]. The indirect driving type is the most common one used in industries. A typical indirect driving wind turbine mainly consists of a rotor, a hub, a main shaft, a gearbox, flexible couplings, and a generator, as shown in Fig. 1.

The time-varying wind load drives blade rotation, which propels the generator through the speed-up gearbox. Wind energy is transformed into electric energy through this process. The speed of the main shaft commonly ranges between 10 and 20 r/min, whereas that of the generator shaft normally ranges between 1000 and 1800 r/min. Fig. 2 depicts the structure of the gearbox sample, which includes a planetary gear stage and two involute gear stages (An intermediate-speed stage and a high-speed stage). The main parameters for the transmission system are listed in Table 1.

Table 1. Main parameters of the gearbox.

Parameters	Planetary stage			Intermediate stage		High-speed stage	
	S	P	I	G	W	G	W
Number of teeth	21	37	96	97	23	103	21
Module /mm	15	15	15	11	11	8	8
Helical angle/°	8	8	8	10	10	10	10
Pressure angle/°	25	25	25	20	20	20	20
Ratio	5.571			4.217		4.905	

Note: *S*- sun gear; *P*- planet gear; *I*- internal gear; *G*- gear; and *W*-wheel.

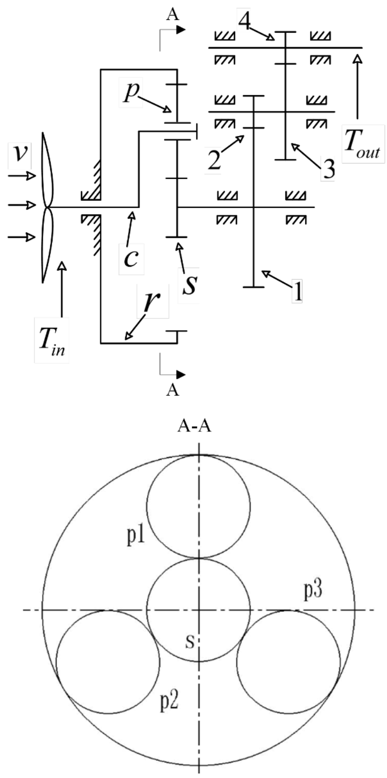

Note: *r*- the internal ring; *c*- the carrier; *p1*, p2, and p3- the planet gears; *s*- the sun gear; 1 and 2- the gear and the wheel of the intermediate gear stage, respectively; and 3 and 4 -the gear and the wheel of the high-speed gear stage, respectively.

Fig. 2. Structure of the speed-up gearbox.

3. Dynamic modeling and analysis

3.1 Dynamic model for the drive train

A coupled lateral—torsional dynamic model was developed for the wind turbine drive train according to the structure of the wind turbine system and to the topological relation among components inside the system. This model is presented in Fig. 3, and the symbols utilized are explained in Table 2.

The support stiffness of effective bearing and time-varying mesh stiffness were considered in dynamic modeling. The shafts of the intermediate- and high-speed gear stages were connected to the housing on the basis of this stiffness. Planet gears were installed in the planet carrier with planet pins. Similarly, the carrier was connected to the housing according to the support stiffness of effective bearing. The ring gear was fixed to the housing. The topological graph of the gearbox for

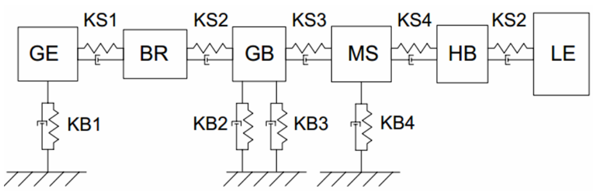

Fig. 3. Dynamic topology of the drive train.

Table 2. Symbols in the topological graph of the drive train.

Symbols	Meaning	Symbols	Meaning
GE	Rotary inertia of the rotating part of the generator	HB	Rotary inertia of the hub
BR	Rotary inertia of the brake (Including the clutch)	LE	Rotary inertia of the leafs
GB	Rotary inertia of the rotating part of the gearbox	KS	Torsional stiffness and damping of shafts
MS	Rotary inertia of the main shaft	KB	Bearing stiffness of the structural components

Table 3. Symbols in the topological graph of the gearbox.

Symbols	C	SG	P	R
Meaning	Planet carrier	Sun gear	Planet gear	Ring gear
Symbols	G	K	B	S
Meaning	Outer gear	Mesh stiffness	Bearing	Shaft

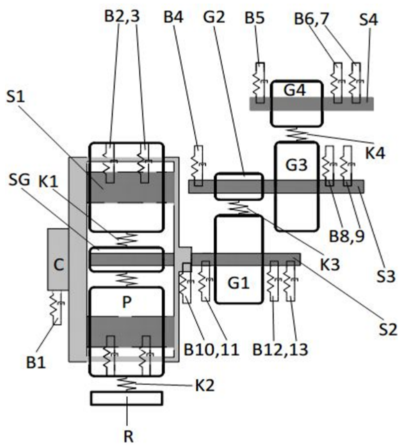

Fig. 4. Topological graph of the gearbox.

dynamic modeling is exhibited in Fig. 4, and the symbols are listed in Table 3.

The blades, main shaft, gear shafts, planetary carrier, and housing of the gearbox are assumed to be flexibilities in dynamic modeling. They are expressed in terms of modal flexibilities. Then, the modal superposition method is applied. The linear combination of the eigenvector and the modal coordinate represents the elastic displacement. To reduce the calculation cost, the method of limiting the dynamic substructure of finite elements is selected to reduce the DOFs of the flexibility bodies. The substructures and super elements are defined, and interface nodes are used to describe the modal characteristics of the flexible bodies.

The commercial package Simpack was used for the calculation in this study to solve the model of rigid-flexible coupled multi-body dynamics. In this model, bearings are represented

Table 4. First 14-order natural frequencies.

Order	1	2	3	4	5
Frequency/Hz	1.72	9.1	184.1	224.3	319.5
Order	6	7	8	9	10
Frequency/Hz	405.2	670.5	1028.3	1125.4	1318.1
Order	11	12	13	14	
Frequency/Hz	1343.5	1408.6	1538.6	1621.7	

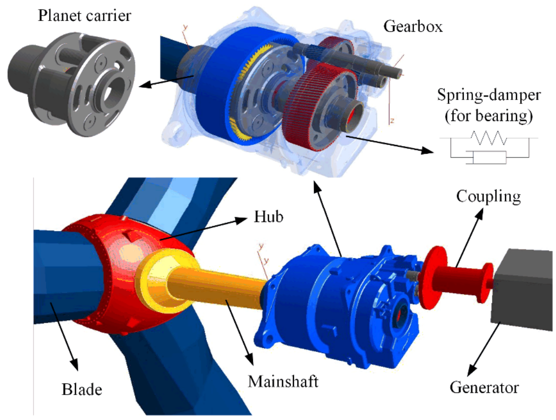

Fig. 5. Dynamic model of the wind turbine drive train.

by springs with five DOFs. The waving and shimmy DOFs of the blades are considered as well. The gear mesh and bearing stiffness of the structural components are provided in Ref. [22] along with the mass and rotary inertial.

3.2 Natural characteristics

The dynamic differential equation of the system can be expressed as

$$[M]\{\ddot{x}\}+[C]\{\dot{x}\}+[K]\{x\}=\{F\}, \tag{1}$$

where M, C, and K are the matrices of the mass, damping, and stiffness of the drive train, respectively. $\ddot{x}$, $\dot{x}$, and x are the vectors of the acceleration, velocity, and displacement of the system, respectively. F is the load vector.

The first 14-order natural frequencies that are applied in the subsequent potential resonance analysis are listed in Table 4 after the proposed systematic dynamic model is solved. The first six-order mode shapes are depicted in Fig. 6. The results show that the first-order natural frequency is 1.72 Hz. This frequency represents a torsional vibration mode. The dynamic characteristic of the system is complicated, and the main vibration modes are the torsional and bending vibrations.

3.3 Potential resonance analysis of the drive train

The main vibration mode of the drive train is torsional vibration. The internal and external excitations of the drive train are mainly observed along the torsional direction. The damp-

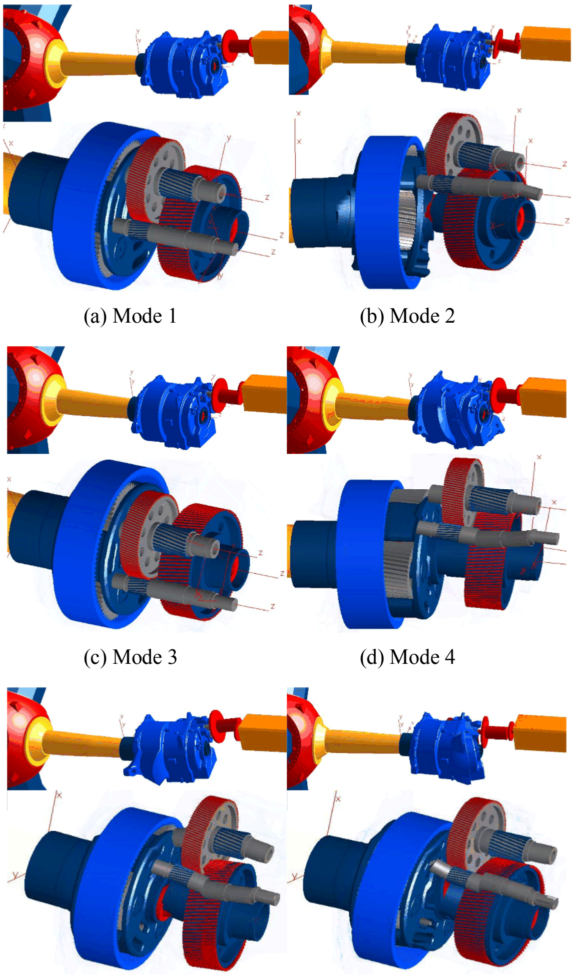

(a) Mode 1 (b) Mode 2

(c) Mode 3 (d) Mode 4

(e) Mode 5 (f) Mode 6

Fig. 6. First six-order mode shapes.

ing along this direction is small, thus indicating that the vibration absorption effect is weak. These factors imply that potential resonances may be observed in the drive train. Such resonances are highly detrimental and dangerous to the machine, and they are discussed in this section. The excitation frequencies (i.e., the rotation frequencies of the shafts and the mesh frequencies of the gear pairs) under different operating speeds are provided in Table 5.

Fig. 7 displays the Campbell diagrams constructed according to Tables 4 and 5. The frequencies with the abbreviations “eign_i” (i = 1–14) represent the natural frequencies of different modes. Several excitation frequencies (i.e., the second-harmonic of the rotating frequencies of the low-speed shafts, as well as the mesh frequencies and the harmonics of these shafts) intersect with the torsional natural frequencies.

Modal energy distribution is strongly related to the vibration strength for the components in the system. A high modal energy represents strong vibrations for the component under the specified excitation. Fig. 8 illustrates the modal energy distributions of the components under the first-order natural frequency. Modal energy is mainly concentrated at the blades, flexible coupling, and generator rotor. The results of the Campbell diagrams in Fig. 7 suggest that the curve of the first-order natural frequency merely intersects with that of the second-harmonic rotating frequency for the intermediate shaft; therefore, the main modal energy point does not coincide with the frequency intersection point. Thus, resonance does not occur under excitation with the first-order natural frequency.

Modal energy distributions are predicted under each natural frequency. Eight orders of natural frequencies are the potential resonance frequencies for the studied drive train. The corresponding relation between the risk and excitation frequencies are presented in Table 6. The results indicate that the risk frequencies are mainly observed around the harmonics of the mesh frequencies at the intermediate stage (between 150 and 350 Hz) and the high-speed stage (between 1000 and 1650 Hz).

Table 5. Excitation frequencies under different speeds.

Different speed r/min	Cut-in speed	Rated speed	Cut-out speed
	1050	1790	1900
ms_1p	0.15	0.26	0.29
ms_2p	0.30	0.52	0.58
ms_3p	0.46	0.78	0.87
lss_1p	0.85	1.44	1.61
lss_2p	1.69	2.88	3.22
lss_3p	2.54	4.33	4.83
ims_1p	3.57	6.08	6.79
ims_2p	7.14	12.17	13.59
ims_3p	10.70	18.25	20.39
hss_1p	17.50	29.83	33.33
hss_2p	35.00	59.67	66.67
hss_3p	52.50	89.50	100
lss_mesh_1p	17.77	30.29	33.84
lss_mesh_2p	35.53	60.57	67.68
lss_mesh_3p	53.30	90.86	101.5
ims_mesh_1p	82.06	139.8	156.3
ims_mesh_2p	164.1	279.7	312.6
ims_mesh_3p	246.1	419.6	468.9
hss_mesh_1p	367.5	626.5	700.0
hss_mesh_2p	735.0	1253.0	1400
hss_mesh_3p	1102	1879	2100

Note: ms_ip- rotational frequency of the main shaft; lss_ip- rotational frequency of the low-speed shaft; ims_ip- rotational frequency of the intermediate shaft; hss_ip- rotational frequency of the high-speed shaft; lss_mesh_ip- mesh frequency of the low-speed gear stage; ims_mesh_ip- mesh frequency of the intermediate-speed gear stage; and hss_mesh_ip- mesh frequency of the high-speed gear stage. Cut-in speed is the minimum speed at which the generator can produce electricity, whereas cut-out speed is the maximum speed. i = 1 for 1st order, i = 2 for 2nd order, and i = 3 for the 3rd order.

Table 6. Risk frequencies and corresponding excitation frequencies.

Order	Risk frequency /Hz	Excitation frequency	Speed r/min
3	184.18	ims_mesh_2p	1110
4	224.36	ims_mesh_2p	1430
5	319.51	ims_mesh_3p	1400
8	1028.3	hss_mesh_2p	1550
9	1125.49	hss_mesh_2p	1620
10	1318.12	hss_mesh_3p	1300
11	1343.59	hss_mesh_3p	1320
14	1621.71	hss_mesh_3p	1600

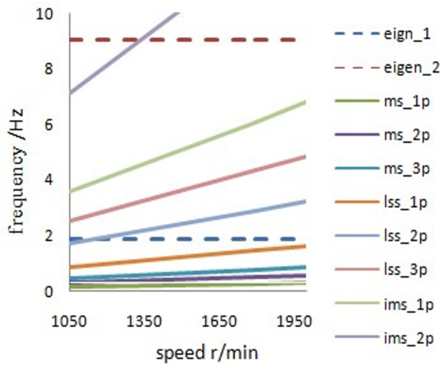

(a) 0–10 Hz

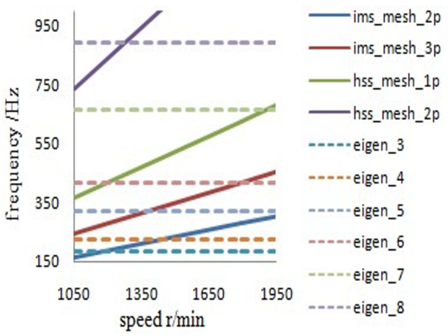

(b) 100–1000 Hz

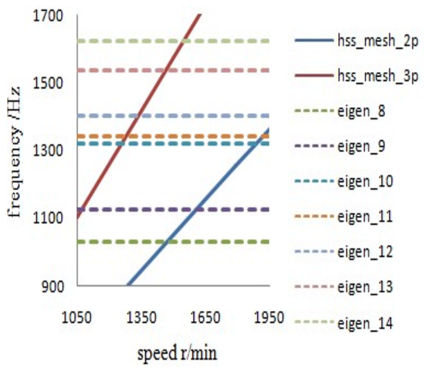

(c) 1000–1900 Hz

Note: eign_i-natural frequencies and i = 1–14 is the order number.

Fig. 7. Campbell diagrams under normal operating conditions.

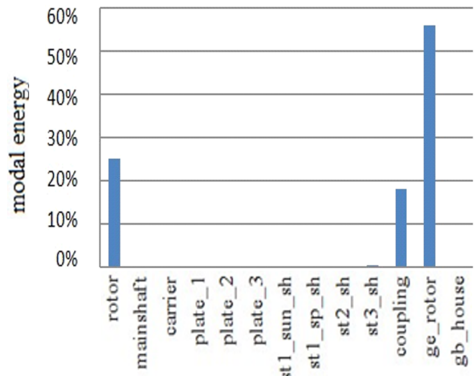

Fig. 8. Modal energy distribution under the first-order natural frequency.

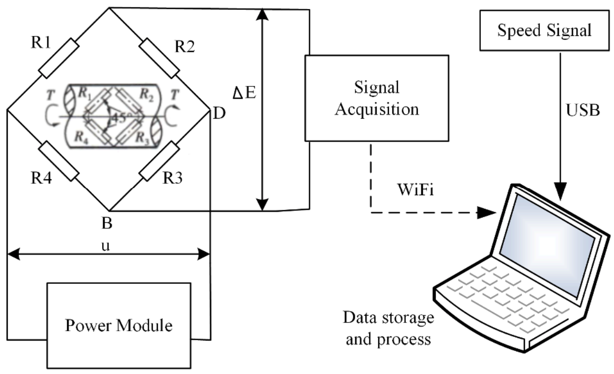

Fig. 9. Block-diagram of the experimental measurement system.

4. Experimental study

An experimental system was developed to test the torsional vibration of the drive train, as shown in Fig. 9. The WiFi data transmission method is applied to this system. In consideration of the actual mounting space requirements, a torque measurement system is installed on the shaft of the generator rotor, and the eddy current speed sensor is installed on the brake disc. The installation processes of the torsional vibration sensor and of the tachometer are depicted in Fig. 10. The basic parameters of the torsional vibration test are provided in Table 7.

The torque signals are recorded during start-up, stop, and normal operations when the wind speed is 4-5 m/s and the rated load is 25%. The signals from the start-up procedure are analyzed using the fast Fourier transform algorithm, as presented in Fig. 11. Fig. 12 displays the torsional vibration under steady state with a generator speed of 1540 r/min.

The results indicate that an impulsive torque was clearly observed during the start and stop processes due to the large inertia mass of the blade. The torque signal in the frequency domain suggests that the torsional frequency is approximately 1.709 Hz. The torsional vibration under steady state peaks at a rotating frequency of 25.6 Hz with a generator speed of 1540 r/min. Thus, the experimental results are consistent with the theoretical simulation results.

Table 7. Basic parameters of the test system.

Strain gage	Model number	Resistance/Ω	Sensitivity coefficient
	BE-120-2HA-E	119.8 ± 0.1	2.19 ± 1%

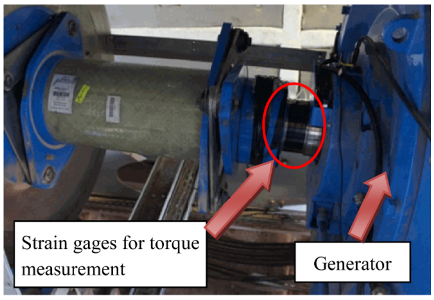

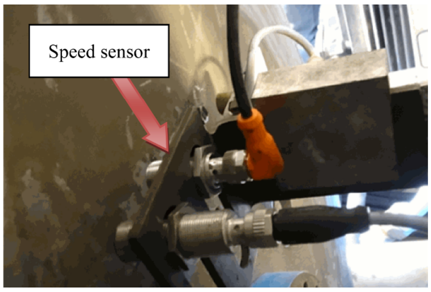

Fig. 10. Location of the torsion vibration and speed sensors.

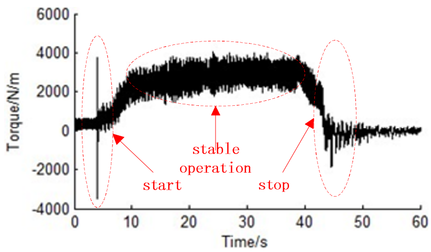

(a) Time-domain curve of the torque

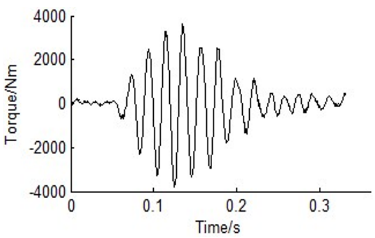

(b) Time-domain curve of the torque during start-up

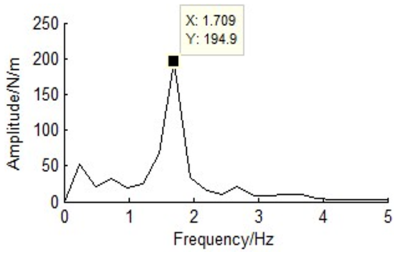

(c) Frequency domain of the torque during start-up

Fig. 11. Torsional vibration of the generator rotor during start-up.

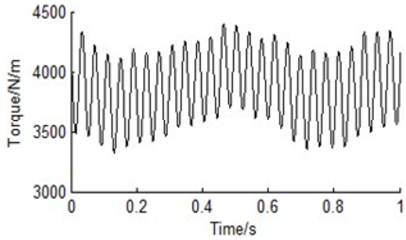

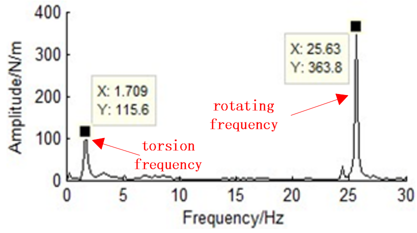

Fig. 12. Torsional vibration of the generator rotor in normal operation.

5. Conclusions

The dynamic model of a MW wind turbine drive train was developed in this work. The blades, hub, main shaft, and gearbox were assumed to be flexible bodies. The method of rigid-flexible coupling multi-body dynamics was applied to develop the dynamic model of the entire drive train. This model was used to determine the natural characteristics of the system. The potential resonances of the system were examined through Campbell analysis and modal energy distribution. The theoretical results show that the first-order natural frequency of the system is approximately 1.72 Hz. This frequency represents a torsional vibration mode. The risk frequencies for this drive train are mainly located around the harmonics of the mesh frequencies of the intermediate- and high-speed gear stages. The amplitudes of acceleration are small; hence, resonances are not observed within the normal operating speed range. To verify the theoretical model, an experimental remote real-time system was developed to monitor the torsional vibration conditions of the drive train. That of the system is tested according to the conditions of the drive train. Torque signals are recorded during start-up, stop, and normal operations. The peak is reached at the first-order natural frequency of the system, which is approximately 1.709 Hz. The experimental results are in accordance with the theoretical results.

Acknowledgment

This work was supported financially by the National Plan for Science and Technology Support of China (2012BAA01B05).

References

[1] A. Hemami, *Wind turbine technology*, Delmar Cengage Learning (2011).

[2] G. Lloyd, *Wind energy GmbH, rules and guide-lines, IV Industrial Services*, Guideline for Certification of Wind Turbines, Supplement (2010).

[3] J. Krouse, Wind turbine gearbox vibration, *Power Engineering*, 113 (10) (2009) 16-17.

[4] C. C. Zhu et al., Analysis of nonlinear coupling dynamic characteristics of gearbox system about wind-driven generator, *Chinese Journal of Mechanical Engineering*, 41 (8) (2005) 203-207.

[5] D. T. Qin, J. H. Wang and T. C. Lim, Flexible, Multibody dynamic modeling of horizontal wind turbine drivetrain system, *Journal of Mechanical Design*, 131 (2009) 114501-1-8.

[6] W. Leithead and M. Rogers, Drive-train characteristics of constant speed HAWT's: Part I-representation by simple dynamic models, *Wind Engineering*, 20 (3) (1996) 149-174.

[7] M. Martins et al., Validation of fixedspeed wind turbine dynamic models with measured data, *Renewable Energy*, 32 (2007) 1301-1316.

[8] K. Stol, Dynamics modeling and periodic control of horizontal-axial wind turbines, *Ph.D. Dissertation*, University of Colorado (2001).

[9] Y. Nam, Y. La, J. Son, Y. Oh and J. Cho, The effect of torque scheduling on the performance and mechanical loads of a wind turbine, *Journal of Mechanical Science and Technology*, 28 (2014)1599-1608.

[10] J. Helsen, P. Peeters, K. Vanslambrouck, F. Vanhollebeke and W. Desmet, The dynamic behavior induced by different wind turbine gearbox suspension methods assessed by means of the flexible multibody technique, *Renewable Energy*, 69 (2014) 336-346.

[11] A. Burlibasa and E. Ceanga, Frequency domain design of gain scheduling control for large wind systems in full-load region, *Energy Conversion and Management*, 86 (2014) 204-215.

[12] B. Song, S. Hu and H. Xu, Application of flexible multibody method for wind turbine drive train dynamic modeling, *Proceedings of the 2013 International Conference on Energy*, Hengshan, China (2013) 250-260.

[13] J. Peeters, D. Vandepitte and P. Sas, Analysis of internal drive train dynamics in wind turbine, *Wind Energy*, 9 (2006) 141-161.

[14] J. Peeters, D. Vandepitte and P. Sas, Flexible multibody model of three-stage planetary gearbox in a wind turbine, *Proc. ISMA*, Leuven (2004) 3923-3941.

[15] C. C. Zhu, X. Y. Xu and H. J. Wang, Modal prediction and sensitivity analysis of wind-turbine planetary gear system with flexible planet pin, *Advanced Science Letters*, 4 (3) (2011) 1219-1224.

[16] C. C. Zhu, X. Y. Xu, T. C. Lim, X. S. Du and M. Y. Liu, Effect of flexible pin on the dyamic behaviors of wind turbine planetary gear drives, *Proceedings of the Institution of Mechanical Engineers, Part C Journal of Mechanical Engineering Science*, 227 (2013) 74-86.

[17] C. C. Zhu, X. Y. Xu and H. J. Liu, Research on dynamical characteristics of wind turbine gearboxes with flexible pins, *Renewable Energy*, 68 (2014) 724-732.

[18] C. C. Zhu, S. Chen, H. J. Liu, H. Q. Huang, G. F. Li and F. Ma, Dynamic analysis of the drive train of a wind turbine based upon the measured load spectrum, *Journal of Mechanical Science and Technology*, 28 (2014) 2033-2040.

[19] B. Marrant, The validation of MBS multi-megawatt gearbox models on a 13.2 MW test rig, *Simpack User Meeting* (2012) 3.

[20] P. Maegaard, A. Krenz and W. Palz, *Wind power for the world: international reviews and developments*, Pan Stanford Publishing Pte Ltd, CRC Press, Boca Raton, United States (2013).

[21] S. Stephan, V. Berbyuk and H. Johansson, *Review on wind turbines with focus on drive train system dynamics*, Wind Energy (2014).

[22] S. Chen, Dynamic characteristics research of megawatt level wind turbine drive train, *Master Thesis*, Chongqing University (2013).

Caichao Zhu is currently a professor at the State Key Laboratory of Mechanical Transmission, Chongqing University, China. His research interests include the dynamics of gear systems, the tribology of mechanical transmissions, and the design of accurate transmission, among others. He has published more than 100 technical papers in international journals.